In vivo imaging of human burn injuries with polarization-sensitive optical coherence tomography

Ki Hean Kim
Mark C. Pierce
Gopi Maguluri
B. Hyle Park
Sang June Yoon
Martha Lydon
Robert Sheridan
Johannes F. de Boer

In vivo imaging of human burn injuries with polarization-sensitive optical coherence tomography

Ki Hean Kim,[a,b] Mark C. Pierce,[c] Gopi Maguluri,[d] B. Hyle Park,[e] Sang June Yoon,[a] Martha Lydon,[f] Robert Sheridan,[f,g] and Johannes F. de Boer[h]

[a]Pohang University of Science and Technology, Department of Mechanical Engineering, Pohang 790-784, Republic of Korea
[b]Pohang University of Science and Technology, Division of Integrative Biosciences and Biotechnology, Pohang 790-784, Republic of Korea
[c]Rutgers, The State University of New Jersey, Department of Biomedical Engineering, Piscataway, New Jersey 08854
[d]Thorlabs Inc., 435 Route 206, Newton, New Jersey 07860
[e]UC Riverside, Department of Bioengineering, Riverside, California 92521
[f]Massachusetts General Hospital, Department of Surgery, Massachusetts 02114
[g]Shriners Hospital for Children, Department of Surgery, Boston, Massachusetts 02114
[h]VU University, Institute for Lasers, Life and Biophotonics Amsterdam, Department of Physics and Astronomy, de Boelelaan 1081, 1081 HV Amsterdam, Netherlands

Abstract. The accurate determination of burn depth is critical in the clinical management of burn wounds. Polarization-sensitive optical coherence tomography (PS-OCT) has been proposed as a potentially non-invasive method for determining burn depth by measuring thermally induced changes in the structure and birefringence of skin, and has been investigated in pre-clinical burn studies with animal models and ex vivo human skin. In this study, we applied PS-OCT to the in-vivo imaging of two pediatric burn patients. Deep and superficial burned skins along with contralateral controls were imaged in 3D. The imaging size was 8 mm × 6 mm × 2 mm in width, length, and depth in the air respectively, and the imaging time was approximately 6 s per volume. Superficially burned skins exhibited the same layered structure as the contralateral controls, but more visible vasculature and reduced birefringence compared to the contralateral controls. In contrast, a deeply burned skin showed loss of the layered structure, almost absent vasculature, and smaller birefringence compared to superficial burns. This study suggested the vasculature and birefringence as parameters for characterizing burn wounds. © *2012 Society of Photo-Optical Instrumentation Engineers (SPIE).* [DOI: 10.1117/1.JBO.17.6.066012]

1 Introduction

Evaluating the depth of burn injuries at the earliest stage is critical for treatment planning and is a major determinant of long term prognosis.[1,2] Mild, superficial burns will heal spontaneously within 2 weeks, but deep burns require active intervention through methods such as skin grafting to promote healing and avoid scar formation. Burn wounds are usually evaluated by visual assessment, the accuracy of which is heavily dependent on the surgeon's expertise. An objective, non-invasive, quantitative method to determine burn depth would significantly impact patient care, particularly in environments where patients lack access to experienced surgeons.

Many methods have been developed for the quantitative evaluation of burn wounds, including biopsy and histopathology,[3,4] laser Doppler flowmetry (LDF) and perfusion imaging,[5–10] ultrasound imaging,[11–13] fluorescence imaging,[14] thermography,[15] reflectance and multispectral imaging,[16,17] magnetic resonance imaging,[18,19] and polarization-sensitive optical coherence tomography (PS-OCT).[20,21] LDF measures changes of perfusion in burn wounds over time, and it is known that burns with different severity show different patterns of perfusion change. LDF has been proved to provide useful information for burn depth

evaluation in clinical studies.[1] LDF is sensitive to various wound conditions such as tissue thickness, presence of edema etc., because it is not a 3D imaging technique.

PS-OCT is also promising due to its ability to provide 3D information on tissue microstructure and birefringence in a non-invasive fashion, to the depth approaching a few millimeters beneath the tissue surface. Birefringence is a useful parameter for the evaluation of burn injury. The dermal layer of skin is composed of extra-cellular matrix (ECM) containing collagen and elastin. Collagen fibers of dermis exhibit strong birefringence due to their characteristic molecular structure and highly ordered arrangement. Upon heating, collagen undergoes a transition from a rod-like alpha helix to a random-coil conformation, resulting in decrease of the native birefringence. This decrease in birefringence due to burn damage was quantified using PS-OCT imaging and correlated to histopathology in the studies of an *in vivo* animal model[20] and ex vivo human skin.[21] Further, multi-functional OCT imaging can provide Doppler flow information as well.[22]

In this study, we extended these earlier PS-OCT burn studies by imaging human burn patients *in vivo*. We conducted 3D PS-OCT imaging at superficial and severe burn sites along with contralateral control sites. These burn sites were characterized in terms of tissue structure including vasculature and tissue birefringence.

Address all correspondence to: Ki Hean Kim, Pohang University of Science and Technology, Department of Mechanical Engineering, Pohang 790-784, Republic of Korea. Tel: +82 542792190; Fax: +82 542793199; E-mail: kiheankim@postech.edu

2 Material and Methods

2.1 Imaging System

We used a spectral domain PS-OCT system, which was described previously in the literature.[22] In brief, the system uses a broadband super-luminescent diode (SLD) with 1320 nm center wavelength and 68 nm bandwidth as a light source, and a polarization modulator in the source arm. The polarization modulator ensured that light in two different polarization states, separated by 90 deg in the Poincare sphere, was incident on the tissue at alternate depth-scans. Conventional OCT intensity images were obtained from the magnitude of backscattered light in each depth scan, with tissue birefringence obtained by analyzing the polarization states of light returning from tissue at the two adjacent depth-scans acquired with different incident polarization states. The imaging speed was 18.5 k depth-scans/s, and the imaging depth was 2 mm in the air with an SNR of approximately 50 dB at the sample surface and 8 dB sensitivity drop-off over this range. Patients were imaged using a custom-made hand-held probe composed of a fiber optic collimator, an x-y scanner, and a lens. This probe had an optical window at the intended working distance in order to maintain the tissue surface close to the zero optical path length difference, and the probe window touched the specimen during imaging. This window was slanted at 8 deg to the normal of incident beam direction in order to avoid collecting strong specular reflection of incident beam from the window surface. During the imaging procedure, both OCT intensity and polarization-sensitive (PS) images were displayed in real time on the computer screen. PS images were displayed as the accumulated phase retardation relative to the tissue surface, using a gray scale ranging from black (0 deg) to white (180 deg).

2.2 Patient Imaging

The study protocol was approved by the Institutional Review Board (IRB) of Massachusetts General Hospital. The PS-OCT system was brought to the operating room or patient room, with patients imaged on the same day as their scheduled clinical evaluation. The hand-held probe (Fig. 1) was covered with a sterile plastic bag, and gently placed onto the skin during imaging. 100 cross-sectional images (in the x-z plane), composed of 1024 depth-scans per image, were acquired with a stepwise increment in the y direction between frames, comprising a 3D image volume covering 8 mm × 6 mm × 2 mm in width (x), length (y), and depth (z) in the air respectively. The imaging time was approximately 6 s per site. Multiple burn sites and their

Fig. 1 Burn imaging scene.

contralateral control sites were imaged. Two patients were imaged at the Shriners Hospital for Children in Boston, which specializes in pediatric burn care. The first patient, a two year-old black American boy, had suffered a hot water burn. This patient was evaluated on day six post-injury, and was imaged on the same day. Five sites were imaged; one was considered by the attending surgeon to be a deep burn site, three sites were considered to be superficial burns, and one site was imaged as a contralateral control. The deep burn site received a skin graft on the day of evaluation. The second study patient was an 11 year-old white American boy whose clothing caught fire. This patient was clinically evaluated on day four post-injury and imaged with PS-OCT on the same day. Ten sites were imaged; five considered by the attending surgeon to be superficial burns and five contralateral controls.

3 Results

We first compared PS-OCT images of a deep burn, superficial burn, and contralateral control of the superficial burn of the first patient (Fig. 2). A 3D reconstructed image and three representative cross-sectional images in the x-z plane at different y locations are shown. Conventional intensity images are shown alongside the corresponding PS images. Intensity images of the contralateral control [Fig. 2(a) and 2(b), Video 1] show the typical layered structure of healthy skin comprising the epithelium and dermis, and some vasculature. PS images of the control show horizontal black-white banding patterns in the cross-sectional images [Fig. 2(b), right], indicating the presence of birefringence. The magnitude of tissue birefringence is proportional to the rate of change in the banding pattern: a rapid change in the accumulated phase retardation with depth indicates high birefringence. A second white band appearing at increased depth relative to the first white band in Fig. 2(b) (right), indicated by arrows, is an artifact: an aliased image of the strongly reflecting surface. Therefore, intensity and phase information lower than the second white band was excluded from subsequent analysis.

Intensity images of the superficial burn [Fig. 2(c) and 2(d), Video 2] show a typical layered skin structure [Fig. 2(d), left] as the contralateral control, and more apparent vasculature than the control. PS images of the superficial burn display reduced birefringence compared to the contralateral control [Fig. 2(d), right], consistent with previous animal and *ex vivo* human studies.[20,21]

Intensity images of the deep burn [Fig. 2(e) and 2(f), Video 3] reveal loss of the layered skin structure, which remained evident in the superficial burn. Tissue vasculature of the deep burn is much less visible than the superficial burn. PS images of the deep burn show much smaller birefringence compared to the superficial burn.

In addition to these qualitative descriptors, tissue birefringence was quantified. Birefringence was measured as the initial slope of accumulated phase retardation with depth into the tissue, consistent with previous analyses.[20,21] Out of 3D data set, birefringence of individual cross-sectional images was analyzed: ranges of valid depth-scans were manually selected in the cross-sectional image based on the criteria that the tissue surface was correctly located and signal was not saturated. These valid depth scans were averaged to yield the accumulated phase retardation of cross-sectional image. The accumulated phase retardation of 3D data set was obtained by calculating the average and standard deviation of those of individual cross-sectional images. The accumulated phase retardations of the superficial burn, its contralateral control, and the deep burn of the first patient
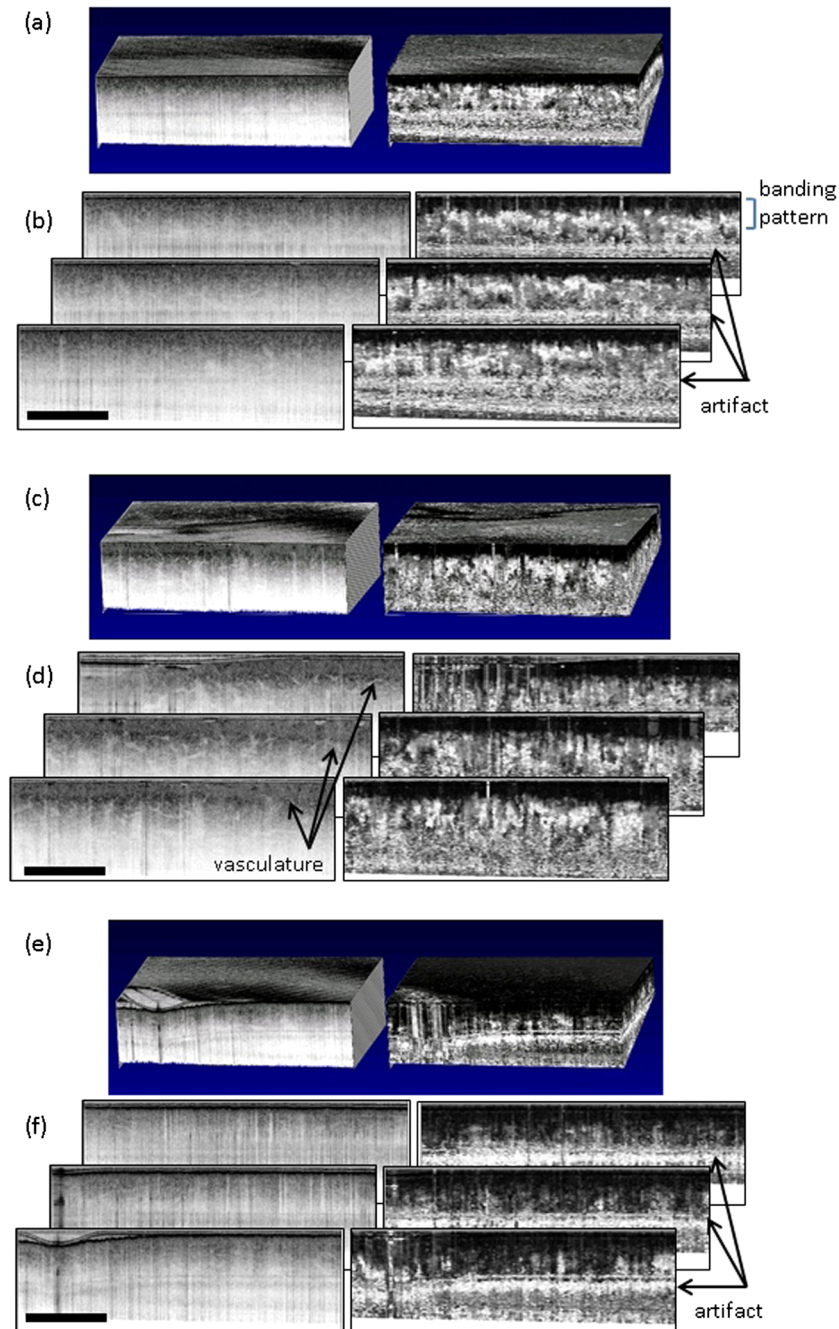
(a)

(b)

banding
pattern

artifact

(c)

(d)

vasculature

(e)

(f)

artifact

Fig. 2 (a & b) PS-OCT images of the contralateral control of a superficial burn (Video 1, QuickTime, 3.0 MB), [http://dx.doi.org/10.1117/1.JBO.17.6 .066012.1] (c & d) the superficial burn (Video 2, QuickTime, 3.2 MB), [http://dx.doi.org/10.1117/1.JBO.17.6.066012.2] (e & f) and a deep burn (Video 3, QuickTime, 2.5 MB) [http://dx.doi.org/10.1117/1.JBO.17.6.066012.3] respectively. A 3D reconstructed image and 3 cross-sectional images are shown in each case, and each PS-OCT image shows an intensity image (left) and PS image (right). The scale bar is 2 mm.

are shown in Fig. 3. These accumulated phase retardation curves were not discrete, due to the averaging process of 3D data sets, which had large spatial variations. The initial slope of the accumulated phase retardation was calculated by selecting an initial linear region manually and by applying a weighted linear least square fit to the region. Initial flat regions of the accumulated phase retardation in both control and superficial burns were due to the presence of epithelium. However, an initial bumpy and flat region in the deep burn was due to the variation of surface finding, and was discarded in the selection of the initial linear region. Calculated initial slope values were

0.73 ± 0.03 deg/μm, 0.43 ± 0.04 deg/μm, and 0.17 ± 0.03 deg/μm for the contralateral control, superficial burn, and deep burn of the first patient respectively (Fig. 3). The measured decrease in birefringence of the superficial burn was significant compared to that of the contralateral control. The deep burn showed smaller birefringence compared to the superficial burn. Superficial burn sites in the second patient were analyzed in the same way: measured initial slopes of the superficial burn/contralateral control sites were 0.26/0.37, 0.31/0.45, and 0.26/0.33 on averages for valid three cases with the standard deviation of less than 0.04. Their unit was degree/μm.
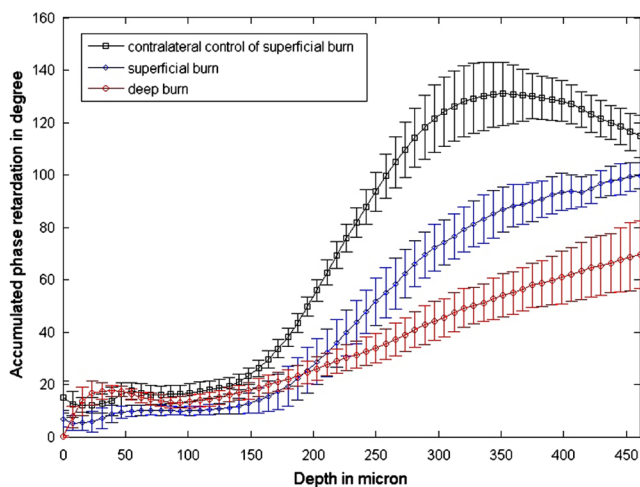
Fig. 3 Accumulated phase retardation with depth of the cases shown in Fig. 2. The error bars are standard deviations of the accumulated phase retardations of cross-sectional images.

PS-OCT images at the superficial burn sites in the first patient showed an additional feature in the vasculature, which may be useful in distinguishing burns of different severities. In order to check whether this feature was consistent in other burn cases, we also investigated superficial burn sites from the second patient (Fig. 4). One representative superficial burn and its contralateral control are shown in Fig. 4(a)–4(c), Video 4, and 4(d)–4(f), Video 5, respectively. The superficial burn [Fig. 4(b) and 4(c)] shows more visible vasculature compared to the contralateral control site [Fig. 4(e) and 4(f)] in both cross-sectional and en-face intensity images. The contralateral control [Fig. 4(e) and 4(f)] shows regular vascular structures that are small in the superficial dermis, becoming larger with depth. In contrast, the superficial burn shows vasculature extending from the superficial dermis without much size change with depth [Fig. 4(b) and 4(c)]. This change of vasculature in the superficial burn may be due to dilation, which needs to be verified with further experiment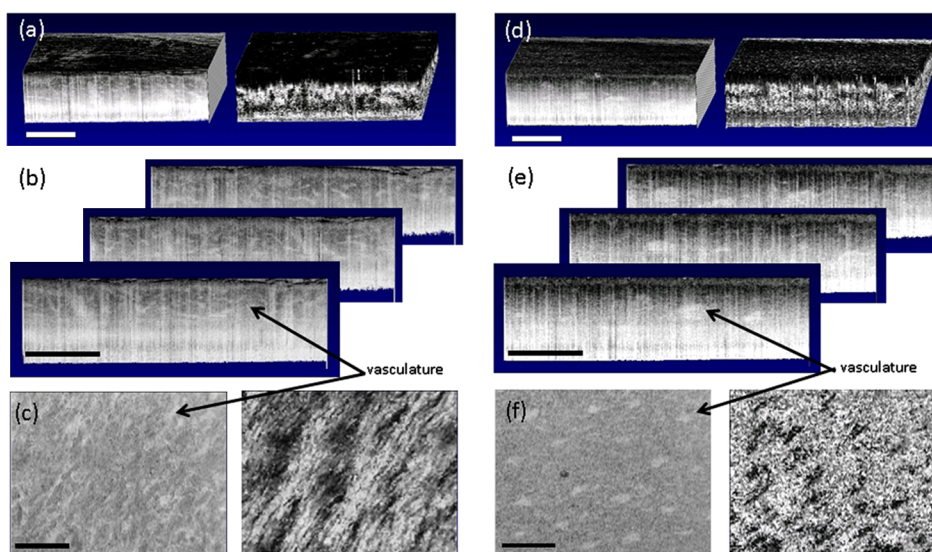s. Other features of superficial burns, such as the presence of layered tissue structure and decrease of birefringence relative to the control, were consistently observed in all cases.

4 Discussion

Volumetric PS-OCT images of burn patient skin were acquired *in vivo*. These data allowed qualitative and quantitative evaluation of tissue structure, vasculature, and birefringence of human skin following deep and superficial burn injury. Superficial and deep burns exhibited qualitative differences in structure, vasculature, and birefringence. Superficial burns were characterized by the appearance of typical layered skin structure and more visible vasculature, with reduced birefringence compared to contralateral controls. The deep burn was characterized by the loss of layered structure, minimal vasculature, and significantly smaller birefringence relative to superficial burns. 3D PS-OCT imaging generated cross-sectional (*x-z*) and en-face (*x-y*) views, providing complementary insights into the spatial distribution of the tissue structure, vasculature, and birefringence, which may prove useful in the characterization of burn severity.

In current practice, patients with small burns are admitted to the hospital and treated with topical care for a few days until it is clear if surgery is needed or not. This delay of decision is related to the fact that burn depth is very often unclear initially; after a few days physical inspection is more reliable than it is initially. If this question ("will the wound heal without surgery?") can be answered earlier with the use of this technique, many hospital days and a great deal of money would be saved.

In this study, we could image only two pediatric patients due to difficulties in patient recruiting. Therefore, this study sufficed to show the potential of PS-OCT in burn depth determination of patients. Further study with more patients needs to be done to validate findings of this study in general burn cases. Nevertheless, this study presents the first data in human subjects and supports the hypothesis that the structural and functional imaging capabilities of PS-OCT may yield a non-invasive, quantitative method for analysis of burn injuries.

Fig. 4 (a–c) Characterization of a superficial burn case of the second patient (Video 4, QuickTime, 2.6 MB) [http://dx.doi.org/10.1117/1.JBO.17.6.066012.4] in comparison with (d–f) its collateral control (Video 5, QuickTime, 3.5 MB). [http://dx.doi.org/10.1117/1.JBO.17.6.066012.5] Each case shows a 3D reconstructed image, 3 cross-sectional intensity images in the *x-z* plane, and an en-face image at the superficial dermal layer in the *x-y* plane. The scale bar is 2 mm.

References

1. S. Monstrey et al., "Assessment of burn depth and burn wound healing potential," *Burns* **34**(6), 761–769 (2008).
2. A. Jaskille et al., "Critical review of burn depth assessment techniques, part I: historical review," *J. Burn Care Res.* **30**(6), 937–947 (2009).
3. M. Ho-Asjoe et al., "Immunohistochemical analysis of burn depth," *J. Burn Care Rehabil.* **20**(3), 207–211 (1999).
4. A. Watts et al., "Burn depth and its histological measurement," *Burns* **27**(2), 154–160 (2001).
5. M. D. Stern, "In vivo evaluation of microcirculation by coherent light scattering," *Nature* **254**(5495), 56–58 (1975).
6. E. Droog, W. Steenbergen, and F. Sjoberg, "Measurement of depth of burns by laser Doppler perfusion imaging," *Burns* **27**(6), 561–568 (2001).
7. S. Pape, C. Skouras, and P. Byrne, "An audit of the use of laser Doppler imaging (LDI) in the assessment of burns of intermediate depth," *Burns* **27**(3), 233–239 (2001).
8. F. Kloppenberg, G. Beerthuizen, and H. J. ten Duis, "Perfusion of burn wounds assessed by laser Doppler imaging is related to burn depth and healing time," *Burns* **27**(4), 359–363 (2001).
9. J. Jeng et al., "Laser Doppler imaging determines need for excision and grafting in advance of clinical judgement: a prospective blinded trial," *Burns* **29**(7), 665–670 (2003).
10. H. Hoeksema et al., "Accuracy of early burn depth assessment by laser Doppler imaging on different days post burn," *Burns* **35**(1), 36–45 (2009).
11. A. Kalus, J. Aindow, and M. Caulfield, "Application of ultrasound in assessing burn depth," *Lancet* **313**(8109), 188–189 (1979).
12. J. Bauer and T. Sauer, "Cutaneous 10 MHz ultrasound B scan allows the quantitative assessment of burn depth," *Burns* **15**(1), 49–51 (1989).
13. S. Iraniha et al., "Determination of burn depth with non-contact ultrasonography," *J. Burn Care Rehabil.* **21**(4), 333–338 (2000).
14. J. Still et al., "Diagnosis of burn depth using laser-induced indocyanine green fluorescence: a preliminary clinical trial," *Burns* **27**(4), 364–371 (2001).
15. F. Wyllie and A. Sutherland, "Measurement of surface temperature as and aid to the diagnosis of burn depth," *Burns* **17**(2), 123–127 (1991).
16. W. Eisenbeiss, J. Marotz, and J. Schrade, "Reflection-optical multispectral imaging method for objective determination of burn depth," *Burns* **25**(8), 697–704 (1999).
17. S. Langer et al., "Assessing the microcirculation in a burn wound by use of orthogonal polarization spectral imaging," *Eur. J. Med. Res.* **6**(6), 231–234 (2001).
18. W. Kudrle, P. Narayana, and H. Dunsford, "Magnetic resonance imaging of burn injury in rats," *Magn. Reson. Imag.* **9**(4), 533–543 (1991).
19. H. Nettelblad, K.-Å. Thuomas, and F. Sjöberg, "Magnetic resonance imaging: a new diagnostic aid in the care of high-voltage electrical burns," *Burns* **22**(2), 117–119 (1996).
20. B. H. Park et al., "In vivo burn depth determination by high-speed fiber-based polarization sensitive optical coherence tomography," *J. Biomed. Opt.* **6**(4), 474–479 (2001).
21. M. C. Pierce et al., "Collagen denaturation can be quantified in burned human skin using polarization-sensitive optical coherence tomography," *Burns* **30**(6), 511–517 (2004).
22. B. H. Park et al., "Real-time fiber-based multi-functional spectral domain optical coherence tomography at 1.3 μm," *Opt. Express* **13**(11), 3931–3944 (2005).